Cruise Control of BLDC Motors Using GA-Optimized Super Twisted Sliding Mode Control

Anwar Hasni [1*], *Hassan* El Fadil[1], *Abdellah* Lassioui[1], *Yassine* El Asri[1], *Marouane* El Ancary[1], *Mohamed Mouyane*[2]

[1]ISA Laboratory, National School of Applied Sciences (ENSA), Ibn Tofail University, Kénitra 14000, Morocco
[2]Laboratoire Universitaire des Sciences Appliquées de Cherbourg (LUSAC), Normandie Univ, UNICAEN, LUSAC, EA 4253, France

Abstract. The rapid development and growing popularity of brushless motors (BLDC) in industrial, automotive and aerospace applications poses a series of inherent challenges, such as precise speed and torque control and, above all, reduced energy efficiency. This work alleviates the above problems by proposing a speed control scheme for brushless motors that takes into account all external disturbances, in particular the variability of load torque with the operating environment. The proposed scheme relies on the use of a controller based on the super-twist sliding mode control strategy (STSMC), whose parameters are optimized using a genetic algorithm (GA). To study the controller's performance and robustness, two test cases were simulated on Matlab/Simulink. The first consisted in verifying tracking performance against a user-specified speed reference value, and the second in checking robustness in the face of an external disturbance, a time-varying load torque. The recorded performances show a motor response time of between 0.02 s and 0.05 s for constant torque, and between 0.02 s and 0.06 s in the presence of disturbances. This performance verifies the robustness and effectiveness of the proposed control strategy, establishing its viability in dynamic operation.

1 Introduction

The rapid expansion of electrical equipment in strategic areas such as industry, electric transport, and aviation brings with it the need for dynamic, intelligent, and efficient drive systems. Brushless direct current (BLDC) drives are characterized by advantages such as high energy efficiency, reduced maintenance thanks to the elimination of brushes, and high-power density [1]. These characteristics make them essential components for applications requiring high dynamic performance, long life, and compactness. Their general application, however, requires overcoming a number of control-related issues, including variable operating environments and external disturbances [2].

Nevertheless, conventional control systems are not sufficient to meet the conditions set by real-life environments, particularly when it comes to dealing with unexpected load changes and external disturbances. These shortcomings most often result in inaccurate speed tracking, instability of the magnet-electric torque, and increased energy absorption, all of

* Corresponding author: hasni.anwar20@gmail.com

which endanger the system's overall performance. It is therefore necessary to develop sophisticated control strategies capable of ensuring optimal motor control, even under variable dynamic conditions and in the presence of disturbances [3].

In literature, several studies have been carried out and different control modes have been introduced with the aim of improving the dynamic performance, precision and robustness to disturbance of brushless motors. Each mode has its specific advantages, but also its shortcomings, depending on the application situation and the target objective. Conventional PID control is still one of the most frequently used, due to its ease of application and good steady-state performance; however, it has serious weaknesses at external difference and large load variations [4]. To overcome these shortcomings, model predictive controls (MPC) have been introduced, with high accuracy due to their function of anticipating future system dynamics, but very sensitive to modeling and requiring a lot of computing power, at the limit of real-time application [5]. At the same time, FOC (Field Oriented Control) vector controls are widely used for the control of synchronous machines, due to their ability to decouple flux and torque control, ensuring fast and efficient response; on the other hand, efficiency depends above all on the quality of position sensors and strict synchronization [6].

Non-linear control methods such as sliding mode control (SMC) have proven to be very robust in the face of disturbances and parametric uncertainties, but they are affected by the phenomenon of chattering, which can lead to unwanted oscillations and premature wear of power electronic devices [7]. To remedy this problem, better versions, such as super-twist mode slip control (STSMC), have been proposed, which significantly reduce chattering while ensuring high robustness and improved control smoothness [8]. At the same time, artificial intelligence has found a basis for presenting intelligent control methods, such as fuzzy logic controllers (FLC), which are capable of controlling imprecise or poorly modeled systems according to simple linguistic rules. The controllers have good flexibility and execution speed, but require empirical rule tuning and sufficiently precise membership functions [9]. Similarly, artificial neural networks (ANNs) are used for their ability to learn the behavior of nonlinear systems from data. Although they can be used to design high-performance adaptive control systems, their training complexity, dependence on data quality and lack of interpretability can be significant limitations [10].

With this point of view, this paper proposes a strong control strategy specific to BLDC motors to ensure reliable and accurate performance, even in the presence of external disturbances and load fluctuations. To this end, the Super-Twisting Mode Gliding control method is used, as it achieves high robustness while reducing the undesirable chattering effects usually associated with traditional SMC methods. To optimize the performance of this controller and adjust its parameters according to operating conditions, off-line parameter optimization is performed using a genetic algorithm. This method achieves an optimum balance between speed, precision and stability of the control system.

After contextualization of the problem addressed and a targeted literature review of current solutions, the remainder of this paper is organized to present the main contributions proposed in a systematic way. Section 2 is devoted to the mathematical modeling of the BLDC motor, detailing the electrical and mechanical equations that define its dynamic behavior. Section 3 presents the control strategy developed, where the principles of STSMC are outlined, in view of its enhanced robustness against uncertainties and disturbances. Section 4 deals with the optimization of controller parameters via a GA, with a clear description of the optimization procedure and the performance criteria used. Section 5 presents the results of simulations carried out in Matlab/Simulink, together with a comparative and critical analysis of the performance obtained using two representative scenarios: following a speed setpoint and rejecting external disturbances, a variable load couple. Finally, the article concludes by summarizing the main contributions of this study and opens up avenues for future research, in particular towards experimental verification.

2 System Modelling

Electromechanical modeling of the BLDC is based on a system of equations describing its electrical, electromagnetic and mechanical dynamics. Each motor phase can be reduced to an RL circuit in series with a trapezoidal counter-electromotive force (FEM) [11]. The voltage equation for a phase is in the form:

$$V_k = R \cdot i_k + L \cdot \frac{di_k}{dt} + e_k \quad \text{with } k = a, b, c \quad (1)$$

where R is the winding resistance, L the phase inductance, i_k the phase current, and e_k the EMF generated by rotor motion.
In matrix form, the three-phase system can be represented by:

$$\begin{bmatrix} V_a \\ V_b \\ V_c \end{bmatrix} = R \begin{bmatrix} i_a \\ i_b \\ i_c \end{bmatrix} + L \cdot \frac{d}{dt} \begin{bmatrix} i_a \\ i_b \\ i_c \end{bmatrix} + \begin{bmatrix} e_a \\ e_b \\ e_c \end{bmatrix} \quad (2)$$

In the most common configurations, the windings are star connected without any neutral ac cessible point, making direct measurement of phase tensions difficult. The line tensions are then used. For instance, the tension between phase A and B is given by:

$$U_{ab} = V_a - V_b = R(i_a - i_b) + L\left(\frac{di_a}{dt} - \frac{di_b}{dt}\right) + (e_a - e_b) \quad (3)$$

The back electromotive force in each phase is proportional to the rotational speed and position of the rotor, according to the relationship:

$$e_k = K_e \cdot \Omega \cdot f_k(\theta) \quad (4)$$

where K_e is the FEM constant, Ω the angular velocity, and $f_k(\theta)$ a trapezoidal function dependent on angular position.
The electromagnetic power generated is given by the sum of the products of the FEM and the currents of each phase:

$$P_{em} = e_a i_a + e_b i_b + e_c i_c \quad (5)$$

This power is transformed into useful mechanical energy, which allows us to express the electromagnetic torque as follows:

$$T_e = \frac{P_{em}}{\Omega} = \frac{e_a i_a + e_b i_b + e_c i_c}{\Omega} \quad (6)$$

In a simplified model, the torque can also be expressed by:

$$T_e = K_t \cdot I \quad \text{or} \quad T_e = \frac{3}{2} \cdot P \cdot \psi \cdot I \quad (7)$$

where K_t is the torque constant, P the number of pole pairs, ψ the maximum magnetic flux, and I the rms current.

The mechanical dynamics of the rotor is modeled by the equation of rotational motion:

$$J \cdot \frac{d\Omega}{dt} + B \cdot \Omega = T_e - T_r \quad (8)$$

where J is the rotor moment of inertia, B the viscous friction coefficient, and T_r the resistive torque.
For frequency analysis and control law design, it is useful to derive a transfer function relating supply voltage to rotor angular velocity [12]. Considering two-phase operation (two active phases at the same time) and assuming r_a=2R, L_a=2(L-M), the electrical equation is written:

$$U_{dc} = r_a \cdot i + L_a \cdot \frac{di}{dt} + K_e \cdot \Omega \quad (9)$$

The current is directly related to the electromagnetic torque by:

$$T_e = K_t \cdot i \quad (10)$$

and the mechanical equation becomes:

$$J \cdot \frac{d\Omega}{dt} + B \cdot \Omega = K_t \cdot i - T_r \quad (11)$$

By Laplace transformation, we obtain the transfer function between speed and input voltage:

$$\frac{\Omega(s)}{U_{dc}(s)} = \frac{K_t}{JL_a s^2 + (Jr_a + BL_a)s + (Br_a + K_e K_t)} \quad (12)$$

The transfer function between angular velocity and resistive torque is also expressed by:

$$\frac{\Omega(s)}{T_r(s)} = \frac{L_a s + r_a}{JL_a s^2 + (Jr_a + BL_a)s + (Br_a + K_e K_t)} \quad (13)$$

These equations form the basis of the BLDC motor dynamic model, enabling the implementation of appropriate control strategies, particularly in environments subject to load disturbances or voltage variations.

3 Cruise Controller Design

This section is devoted to the design of the super-twisting sliding mode controller applied in this work. The proposed approach is divided into two complementary subsections. The first is devoted to the mathematical formalization of the operating principle of the STSMC controller, providing the dynamic equations and control laws involved. The second sub-section is responsible for defining the optimization algorithm used to calculate the controller's two parameters. To this end, a genetic algorithm is used to optimize system performance as far as possible in terms of response rate and robustness.

3.1 Principle and equations of Super-Twisting Sliding Mode Control

The BLDC motor, although powerful, is strongly influenced by load variations, parametric uncertainties, and external disturbances. To ensure robust speed control, especially in dynamic environments, it makes sense to implement a disturbance-tolerant control strategy [13], [14]. The STSMC controller is particularly well suited to this task, combining robustness, fast convergence time, and reduction of the chattering phenomenon often observed in conventional sliding mode controls.
STSMC control is based on the definition of a slip surface s(t) as a function of the speed

error between the setpoint Ω_{ref} (t) and the measured speed Ω(t):

$$s(t) = \frac{d}{dt}e(t) + \lambda e(t) = \dot{e}(t) + \lambda e(t) \quad \text{with } e(t) = \Omega_{ref}(t) - \Omega(t) \quad (14)$$

where $\lambda>0$ is a convergence parameter chosen to guarantee the stability of the surface dynamics.
The second-order STSMC control is then defined by a super-torsion law in the form:

$$u(t) = -k_1|s(t)|^{1/2} \cdot \text{sign}(s(t)) - k_2\int \text{sign}(s(t))\,dt \quad (15)$$

where:
u(t) is the command to be applied (here, proportional to voltage U_{dc}),
$k_1>0$, $k_2>0$ are the super-twisting gains chosen according to system dynamics,
sign(s) is the sign function [15].

This strategy allows finite convergence to the surface s=0 without high-frequency oscillations, while ensuring robust rejection of disturbances T_r (t) or variations in the parameters J, B, K_t, etc.

Practical implementation requires estimation of the derivative term $\dot{e}$(t), which can be achieved using a discrete-time derivative filter, or by adaptive observation methods. Once the control signal has been calculated, it is applied via the bus voltage U_{dc} (t), thus indirectly controlling motor torque and speed.

3.2 Optimization of STSMC parameters using genetic algorithms

In order to improve the dynamic performance of the BLDC motor speed control system, the STSMC controller parameters, in this case the feedback coefficients k_1 and k_2, are optimized using a genetic algorithm. The main objective of this optimization is to minimize speed tracking errors by reducing certain performance criteria that are well established in the literature [16], such as:

- IAE (Integral of Absolute Error):

$$IAE = \int_0^T |\,e_1(t)|\,dt \quad (16)$$

- ISE (Integral of Squared Error):

$$ISE = \int_0^T e_1^2\,(t)\,dt \quad (17)$$

- ITAE (Integral of Time-weighted Absolute Error):

$$ITAE = \int_0^T t \cdot |e_1(t)|\,dt \quad (18)$$

In this study, the ITAE index is preferred as the objective function, as it strongly penalizes prolonged errors, thus favoring rapid response with reduced overshoot. The cost function to be minimized is therefore defined by:

$$J = \int_0^T t \cdot |\Omega_{ref}(t) - \Omega(t)|\,dt \quad (19)$$

The genetic algorithm is applied to find the optimal values of k_1 and k_2 that minimize this function. The optimization process follows the following steps:
Generation of an initial random population of candidate solutions where each individual encodes a pair of payoffs (k_1, k_2).
Evaluation of the cost function J for each individual.
Selection of the best individuals according to their performance.
Application of genetic operations: crossover and mutation, to generate new solutions.
Repetition of the evolutionary process until convergence towards optimal coefficient values.

4 Results and discussion

This section presents a detailed analysis of BLDC motor speed control using an optimized super-twist sliding mode controller. Modeling and simulation were carried out with Matlab software, using the Simulink platform, to efficiently simulate the dynamic response of the system. Two situations were considered for validating the controller's performance: the first to test the system under nominal operating conditions, and the second to enable us to observe its robustness in relation to external disturbances and load changes. The parameters adopted for this simulation are shown in Table 1 below. The parameters found by the offline optimization algorithm used in this simulation are shown in table 2.

Table 1. Parameters for the simulation

Designation	Value
V_{DC}	300 V
R	1.5 Ω
L	0.0115 H
M	0.005 H
K_t	60.3e-3
K_e	60.3e-3
J	0.001 $Kg.m^2$
B	0.002 N.m

Table 2. STSMC optimized controller parameters

Parameters	Value
K_1	92.235348
K_2	100.265591

4.1 First scenario: tracking performances

The main objective of this test scenario is to verify the tracking performance of the optimized STSMC controller. As shown in Figure 1, the reference speed is progressively modified according to the values [500, 800, 1000, 1200] rpm. The dynamic response of the system is marked by excellent transient behavior: the response time in the increasing phases of the setpoint varies from 0.02 s to 0.04 s, while in the decreasing phase from 0.05 s to 0.06 s. It can be clearly observed that the motor speed closely follows the applied setpoint, with the speed error of less than 0.05 s adjusted to zero after each change, as shown in Figure 2.
Figure 3 shows the electromagnetic torque produced by the motor during speed changes. This torque is systematically greater than the load torque, thus effectively compensating for losses due to viscous friction and ensuring robust control. And in case of charge couple, this remains constant to a value of 1 unit (1 Nm) during the test, as indicated by Figure 4. Finally, Figure 5 shows the command tension produced by the controller versus the variation of velocity setpoint. It can be seen that this tension auto-adapts in an effort to achieve tracking of desired speed. According to the relationship of proportionality between rotation speed and input voltage, the controller supplies tensions of order 30 V, 35 V, 40 V and 45 V respectively to speeds of 500, 800, 1000 and 1200 tr/min, hence indicating efficient energy management for precise and fast control of the motor.

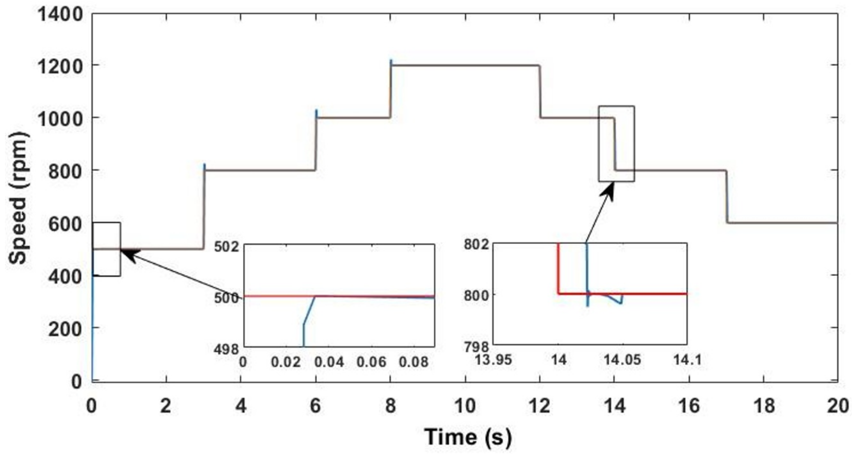

Fig .1. Motor speed changes when the speed control setpoint is changed.

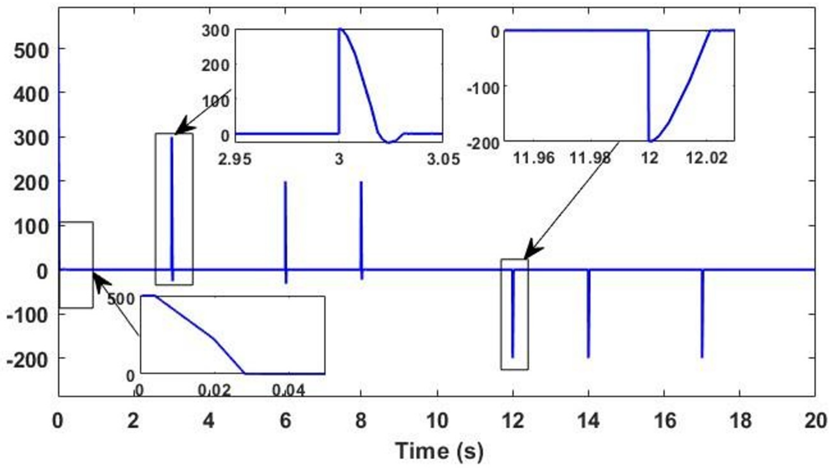

Fig .2. Speed tracking error.

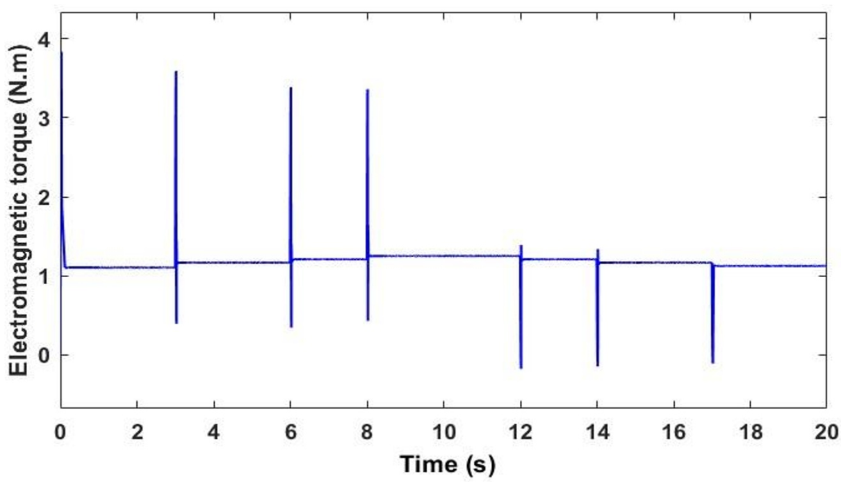

Fig .3. The motor torque generated during reference speed variation.

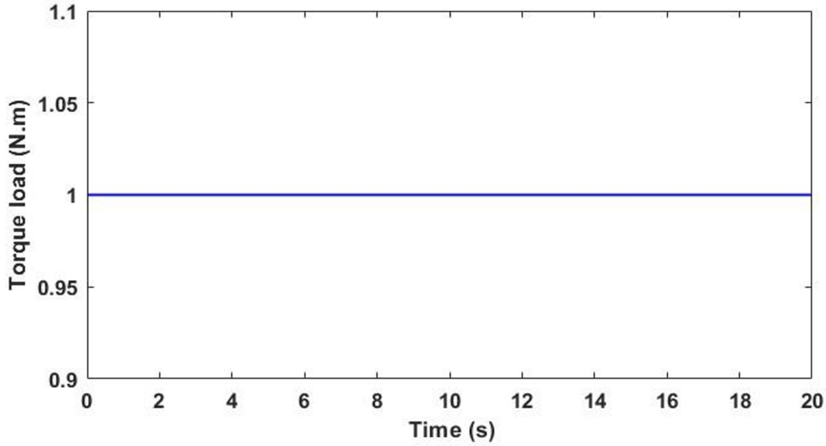

Fig .4. The load torque applied to the motor.

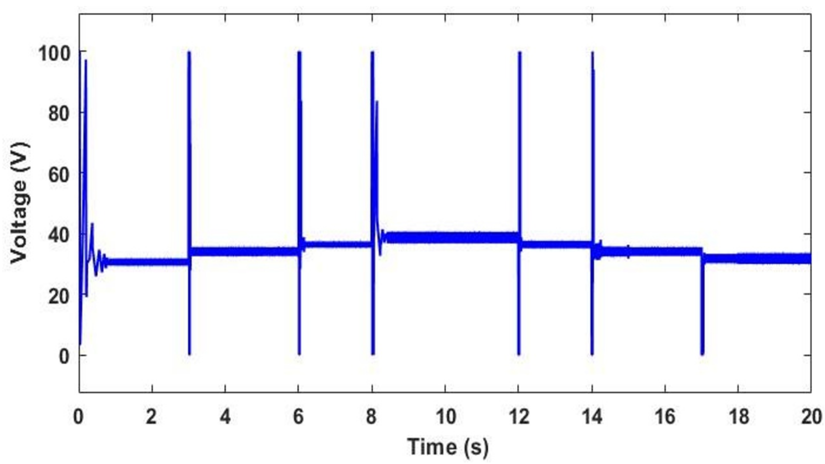

Fig .5. Controller output voltage during speed reference variations

4.2 Second scenario: robustness performances

To test the controller's robustness to load torque variations, a test scenario was set up in which the load torque is varied linearly from the set values [0, 1, 2, 3] Nm, as shown in figure 9. Despite these mechanical disturbances, Figure 6 shows that the motor speed is ideally controlled at the set value of 1000 rpm, demonstrating the robustness and stability of the controller in relation to changing loads. Figure 7 shows that the speed error is always virtually zero for the entire test duration, testifying to the accuracy of the setpoint tracking. In addition, Figure 8 shows that the electromagnetic torque developed by the motor is always higher than the load torque applied, enabling effective compensation of losses caused by friction and disturbances. Finally, Figure 10 shows the output voltage generated by the controller. It can be seen that the motor supply voltage varies dynamically, from 16 V to 82 V, depending on the torque levels applied. Specifically, voltages of around [16 V, 38 V, 59 V, 82 V] are generated for respective load torques of [0, 1, 2, 3] Nm, demonstrating the controller's flexibility in maintaining system performance under variable conditions.

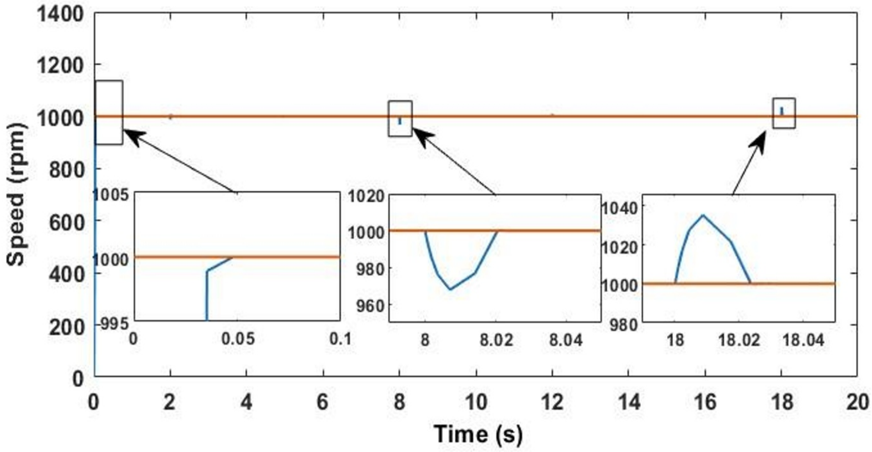

Fig .6. The motor speed variations during change in the load torque.

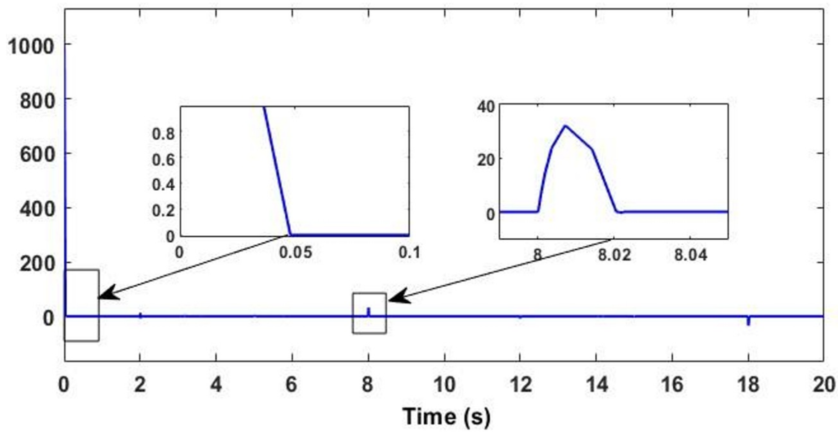

Fig .7. Speed error due to load torque variation

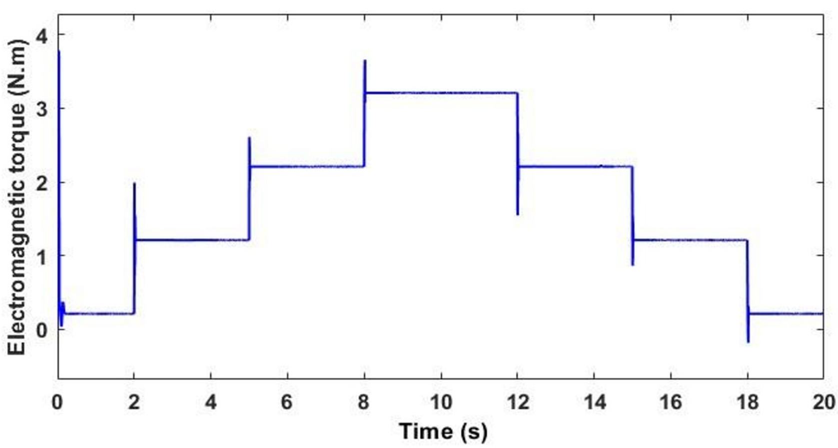

Fig .8. The load torque developed by the motor at the moment of load torque variation

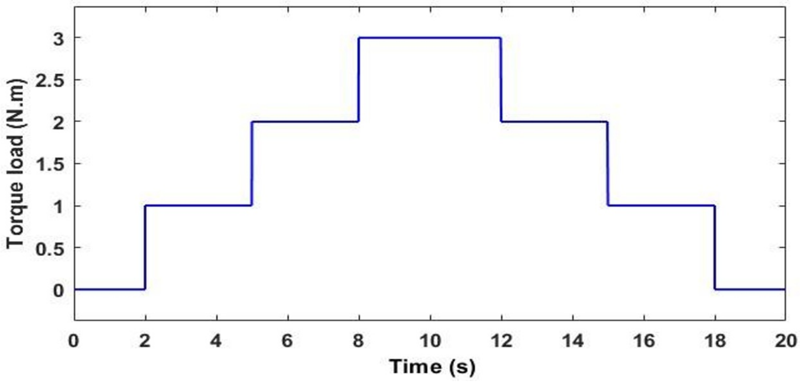

Fig .9. Variable load torque applied to the motor

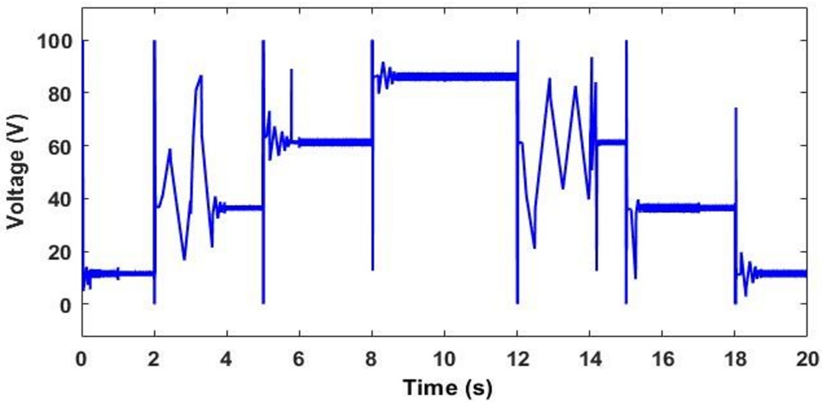

Fig .10. The controller output voltage during change in the load torque

5 Conclusion and perspectives

This paper presents an advanced method of controlling the speed of a BLDC motor for electric vehicles using a high-performance controller based on the Super-Twisting sliding mode control technique optimized to cope with variable loads. The BLDC motor model is implemented using this robust controller to achieve effective speed control, even in the presence of intense load torque fluctuations. The proposed system was subjected to a series of intensive tests through simulations carried out in the MATLAB/Simulink environment, underlining the strength and precision of the STSMC controller. The latter demonstrated a very good ability to maintain constant motor speed under disturbed conditions and to provide fast dynamic behavior. STSMC controller parameters were optimized on the basis of the time-weighted absolute error integral criterion, which minimizes tracking error while penalizing slow responses. This optimization criterion led to a significant improvement in the system's transient performance, reducing both response time and overshoot amplitude. Simulation results show a response time of between 0.02 s and 0.06 s, both under constant load conditions and under dynamic disturbances. This behavior confirms the excellence of the ITAE-optimized STSMC controller in terms of stability, robustness and precision. Future research will include experimental validation on a real test bench to determine the viability of the proposed solution. In addition, the integration of techniques derived from artificial intelligence, such as neural networks or reinforcement learning, will further enhance the controller's flexibility in complex and dynamic environments.

References

[1] K. Kroičs et A. Būmanis, « BLDC Motor Speed Control with Digital Adaptive PID-Fuzzy Controller and Reduced Harmonic Content », *Energies*, vol. 17, nº 6, p. 1311, 2024.

[2] Z. A. Al-Dabbagh et S. W. Shneen, « Design of a PID Speed Controller for BLDC Motor with Cascaded Boost Converter for High-Efficiency Industrial Applications. », Int. J. Robot. Control Syst., vol. 5, no 1, 2025.

[3] H. Sarma et A. Bardalai, « An intelligent PID controller tuning for speed control of BLDC motor using driving training-based optimization », Int. J. Power Electron. Drive Syst. IJPEDS, vol. 14, no 4, p. 2474-2486, 2023.

[4] S. N. Rao, B. M. K. Kumar, B. M. Manjunatha, et A. S. Kumar, « Modified invasive weed optimization MPPT approach for PV system interfaced with BLDC motor for water pumping system », J. Eng. Appl. Sci., vol. 72, no 1, déc. 2025, doi: 10.1186/s44147-025-00651-7.

[5] S. Kaul, N. Tiwari, S. Yadav, et A. Kumar, « Comparative Analysis and Controller Design for BLDC Motor Using PID and Adaptive PID Controller », Recent Adv. Electr. Electron. Eng. Former. Recent Pat. Electr. Electron. Eng., vol. 14, no 6, p. 671-682, nov. 2021, doi: 10.2174/2352096514666210823152446.

[6] D. Joshi, D. Deb, et A. K. Giri, « MRAS disturbance observer-based sensorless field-oriented backstepping control of BLDC motor drive », Electr. Eng., vol. 106, no 5, p. 6681-6701, oct. 2024, doi: 10.1007/s00202-024-02378-9.

[7] J. W. Chan, « Sliding Mode Control of Brushless DC Motor Speed Control », Malays. J. Sci. Adv. Technol., p. 188-193, 2022.

[8] Z. Zhang et Y. Li, « An AEFA-Based optimum design of fuzzy PID controller for attitude control flywheel with BLDC motor », Aerospace, vol. 9, no 12, p. 789, 2022.

[9] P. D. S. et S. K. R., « Artificial Neural Network with Optimized FOPID for Speed Control of Sensorless BLDC Motor Drive », Cybern. Syst., p. 1-23, déc. 2022, doi: 10.1080/01969722.2022.2148920.

[10] R. Sehab, A. Akrad, Y. Saadi, R. Sehab, A. Akrad, et Y. Saadi, « Super-Twisting Sliding Mode Control to Improve Performances and Robustness of a Switched Reluctance Machine for an Electric Vehicle Drivetrain Application », Energies, vol. 16, no 7, avr. 2023, doi: 10.3390/en16073212.

[11] R. Carter S. B. et T. S., « Regenerative Braking in PV-Mounted Electric Vehicle With Reduced Switch VSI-Driven BLDC Motor and HAP-FUP Controller », Int. Trans. Electr. Energy Syst., vol. 2024, no 1, janv. 2024, doi: 10.1155/etep/6465530.

[12] A. Hasni et al., « Reinforcement Learning-Based Control Strategy for BLDC Motors », J. Eur. Systèmes Autom., vol. 58, no 6, juin 2025, doi: 10.18280/jesa.580603.

[13] K. Guo, M. Yang, X. Li, P. Shi, et P. Wang, « Research on a new adaptive integral sliding mode controller based on a small BLDC », IEEE Access, vol. 10, p. 73204-73213, 2022.

[14] R. Shenbagalakshmi, S. K. Mittal, J. Subramaniyan, V. Vengatesan, D. Manikandan, et K. Ramaswamy, « Adaptive speed control of BLDC motors for enhanced electric vehicle performance using fuzzy logic », Sci. Rep., vol. 15, no 1, p. 12579, 2025.

[15] X. Zhao, Y. Gong, H. Jin, et C. Xu, « Adaptive super-twisting-based nonsingular fast terminal sliding mode control of permanent magnet linear synchronous motor », Trans. Inst. Meas. Control, vol. 45, no 16, p. 3057-3066, déc. 2023, doi: 10.1177/01423312231162782.

[16] M.-G. Gustavo et R. Jorge, « Super-twisting speed control of a brushless direct current motor with back-emf », IEEE Lat. Am. Trans., vol. 18, no 12, p. 2055-2062, 2021.